(Hydrosilyl)tungsten Complexes of the Type $(C_5Me_5)(OC)_2(Me_3P)W-SiR_3$ (SiR_3 = SiH_3, $Si(H)_2Me$, $Si(H)Me_2$, Si(H)(Cl)Me, $Si(H)Cl_2$): Synthesis, Crystal Structure, and Detailed Vibrational Analysis

Siegfried Schmitzer,[†] Udo Weis,[†] Harald Käb,[†] Wolfgang Buchner,[†] Wolfgang Malisch,*[,†] Thomas Polzer,[‡] Uwe Posset,[‡] and Wolfgang Kiefer*[,‡]

Institut für Anorganische Chemie, Universität Würzburg, Am Hubland, W-8700 Würzburg, Germany, and Institut für Physikalische Chemie, Universität Würzburg, Marcusstrasse 9-11, W-8700 Würzburg, Germany

Received January 24, 1992

Novel functional silyltungsten complexes of the type $(C_5Me_5)(OC)_2(Me_3P)W-SiR_3$ (SiR_3 = Si(H)Me_2 (**3a**), Si(H)(Cl)Me (**3b**), $Si(H)Cl_2$ (**3c**)) have been prepared by the reaction of the lithium metalate, $Li[W(CO)_2(PMe_3)C_5Me_5]$ (**2**), with the corresponding chlorosilanes in cyclohexane. Treatment of **3b,c** with $LiAlH_4$ provides the hydrosilyl complexes $(C_5Me_5)(OC)_2(Me_3P)W-Si(H)_2R$ (R = Me (**4a**), H (**4b**)) in remarkably good yields. Spectroscopic properties of **3a-c** and **4a,b** have been extensively studied by means of NMR, IR, and especially Raman spectroscopy. In addition the crystal structure has been determined for **4a,b**. Crystal data for **4a**: orthorhombic, *Pbca*, with a = 14.165 (4) Å, b = 15.244 (4) Å, c = 18.596 (4) Å, V = 4015 (3) Å^3, Z = 8, R = 0.032, and R_w = 0.021. Crystal data for **4b**: orthorhombic, $P2_12_12_1$, with a = 8.817 (3) Å, b = 14.449 (4) Å, c = 15.132 (5) Å, V = 1928 (2) Å^3, Z = 4, R = 0.037, and R_w = 0.025. The coordination geometry of **4a,b** is that of a Cp-capped square pyramid with the silyl and the Me_3P ligands in trans positions and a W-Si bond distance of 2.559 (2) Å (**4a**) or 2.533 (3) (**4b**), respectively.

Introduction

Functionalized metallosilanes[1] L_nM-SiR_2X (X = H, halogen) are of interest with respect to nucleophilic or radical exchange reactions involving the metalated silicon atom (a), the generation of cationic silylene complexes via hydride or halide abstraction (b), and the synthesis of silicon-bridged clusters (c).[2] In the case of (a) and (b) a reasonably stable M-Si bond is necessary in order to prevent M-Si bond cleavage during the ligand exchange (a) or in the formed silylene complex (b).

In a series of studies we have demonstrated[3] that ferriosilanes $Cp(OC)_2Fe-Si(R)_2X$ (X = H, Cl; Cp = C_5H_5) are suitable substrates for controlled exchange at the silicon affording ferriohydrosilanes,[4a] -aminosilanes,[4b] -silanols,[4c] -alkoxysilanes,[3] or -azidosilanes[4d] or bis(ferrio)silanes,[4e] respectively. Analogous experiments concerning metallosilanes of the chromium series $Cp(OC)_3M-Si(R)_2X$ (M = Cr, Mo, W) have failed due to insufficient strength of the M-Si bond. Interaction of this species with hydride reagents, dialkylamines, or water cause preferred displacement of the transition metal group leading to the formation of the silicon-free metal product $[Cp(OC)_3M]^-$ or $Cp(OC)_3MH$.[5,6] An effective way to stabilize the M-Si bond in silyl metal complexes involves the introduction of ligands characterized by a high σ-donor/π-acceptor ratio at the transition metal center.[7] Applying this approach, we have modified the silyltungsten species $Cp(OC)_3W-Si(R)_2X$ via replacement of the Cp ligand by the Cp* moiety (Cp* = C_5Me_5) and one of the CO groups by trimethylphosphine.

In this paper we report high-yield syntheses of the functionalized tungsten-silanes $Cp^*(OC)_2(Me_3P)W-SiR_1R_2H$ (R_1, R_2 = Me, Cl) via the alkaline salt route using the novel transition metal anion $[Cp^*(OC)_2(Me_3P)W]^-$. By means of controlled Cl/H-exchange reactions at the silicon using $LiAlH_4$, a first proof is given that the tungsten-silanes prepared are attractive materials to modify the ligand combination concerning the silicon. In addition full structural and spectroscopic characterizations are given for the novel tungsten-silanes with emphasis on Raman spectroscopic results. A comprehensive vibrational analysis is performed, and comparisons with related complexes are also given.

Experimental Section

General Information and Instrumentation. ^1H-, ^{13}C-, ^{31}P-, and ^{29}Si-NMR spectra were recorded on Varian T60, Jeol FX 90Q (FT), Bruker AC 200, and Bruker AMX 400 spectrometers. $\delta(^{31}P)/\delta(^{29}Si)$ chemical shifts were measured relative to external 85% $H_3PO_4/(CH_3)_4Si$. The residual proton and ^{13}C solvent signals of d_6-benzene, d-chloroform, or d_8-tetrahydrofuran, respectively, have been used as an internal reference for the ^1H-NMR and ^{13}C-NMR spectra. Shifts downfield from the standard were assigned positive δ's.

[†] Institut für Anorganische Chemie.
[‡] Institut für Physikalische Chemie.

(1) First results concerning this paper have been presented in: (a) Schmitzer, S.; Wekel, H.-U.; Malisch, W. XXVIIIth International Conference on Coordination Chemistry, Gera, Germany, 1990; abstract of papers, pp 4-30. (b) Schmitzer, S.; Malisch, W. IXth FECHEM Conference of Organometallic Chemistry, Heidelberg, Germany, 1991; abstract of papers, p 24.

(2) (a) Aylett, B. J. *Adv. Inorg. Chem. Radiochem.* **1982**, *25*, 1. (b) Don Tilley, T. In *The Chemistry of Organosilicon Compounds*; Patai, S., Ed.; J. Wiley and Sons Ltd.: New York, 1989. (c) Cundy, C. S.; Kingston, B. M.; Lappert, M. F. *Adv. Organomet. Chem.* **1973**, *11*, 253. (d) Corey, J. Y. *J. Organomet. Chem.* **1986**, *313*, 1. (e) Schubert, U. *Transition Met. Chem.* **1991**, *16*, 137.

(3) (a) Malisch, W.; Thum, G.; Wilson, D.; Lorz, P.; Wachtler, U.; Seelbach, W. In *Silicon Chemistry* (Proceedings of the VIIIth International Symposium on Organosilicon Chemistry, St. Louis, MO); Ellis Horwood: Chichester, U. K., 1988; p 327. (b) Malisch, W.; Käb, H.; Wachtler, U.; Hindahl, K.; Schmitzer, S.; Kaupp, G. XXIV Organosilicon Symposium of the American Chemical Society, El Paso, TX, 1991; abstract of papers, p 15.

(4) (a) Wekel, H.-U.; Malisch, W. *J. Organomet. Chem.* **1984**, *264*, C10. (b) Thum, G.; Malisch, W. *J. Organomet. Chem.* **1984**, *264*, C5. (c) Käb, H.; Malisch, W.; Huch, V.; Veith, M. Submitted for publication. (d) Wachtler, U.; Matreux, J.; Kolba, E.; Malisch, W. *J. Organomet. Chem.* **1989**, *363*, C36. (e) Ries, W.; Malisch, W. *Chem. Ber.* **1979**, *112*, 1304.

(5) (a) Malisch, W.; Kuhn, M. *Chem. Ber.* **1974**, *107*, 979. (b) Malisch, W.; Kuhn, M. *Chem. Ber.* **1974**, *107*, 2835. (c) Malisch, W. *Chem. Ber.* **1974**, *107*, 3835. (d) Hagen, A. P.; Higgins, C. R.; Russo, P. J. *Inorg. Chem.* **1971**, *10*, 1657.

(6) Schmitzer, S.; Ries, W.; Wekel, H.-U.; Malisch, W. To be published.

(7) Lichtenberger, D. L.; Rai-Chaudhuri, A. *J. Am. Chem. Soc.* **1991**, *113*, 2923.

0020-1669/93/1332-0303$04.00/0

Table I. Crystal Data for $Cp^*(OC)_2(Me_3P)W-Si(H)_2Me$ (**4a**) and $Cp^*(OC)_2(Me_3P)W-SiH_3$ (**4b**)

	4a	**4b**
formula	$C_{16}H_{29}O_2PSiW$	$C_{15}H_{27}O_2PSiW$
MW	496.32	482.29
space group	*Pbca* (No. 61)	$P2_12_12_1$ (No. 19)
a, Å	14.165 (5)	8.817 (3)
b, Å	15.244 (4)	14.449 (4)
c, Å	18.596 (4)	15.132 (5)
α, deg	90	90
β, deg	90	90
γ, deg	90	90
V, Å^3	4015 (3)	1928 (2)
Z	8	4
d_{calcd}, g cm^{-3}	1.65	1.66
T, °C	25	−80
μ, cm^{-1}	71.9	62.6
radiation (λ, Å)	Mo Kα (0.710 69) from graphite monochromator	
transm factor (max/min)	0.995/0.745	0.979/0.961
R[a]	0.032	0.021
R_w[b]	0.037	0.025

[a] $R = \sum||F_o| - |F_L||/\sum|F_o|$. [b] $R_w = [\sum w(|F_i| - |F_L|)^2/\sum w|F_o|^2]^{1/2}$.

Infrared spectra were recorded on a Perkin-Elmer 283 grating spectrometer. The solutions were measured in NaCl cells with a 0.1 mm path length which have been purged with nitrogen prior to filling. The resolution was about 2 cm^{-1}.

To accelerate the reaction rate in preparing $Cp^*(OC)_2(Me_3P)W-H$ (**1**), a quartz lamp, TQ 718, 700 W (Hanau), was used for irradiation.

Difference Raman spectra were recorded in a classical 90° arrangement, using the divided spinning-cell technique developed by Zimmerer and Kiefer.[8] The 676.442-nm line of a Spectra Physics Model 2025 Kr^+ laser was used as an exciting source with 100-mW power on the samples. The scattered light was analyzed with a Spex Model 1404 double monochromator and detected by a cooled Burle Model 31034-02A photomultiplier and a photon-counting AT computer system. Plasma lines from the laser tubes were filtered out by means of a modified Anaspec prism filter. The spectral resolution was 3 cm^{-1}. The spectral intensity was corrected by calibration with a tungsten lamp. The spectra were taken from 0.25 M CH_2Cl_2 solutions.

Crystals suitable for diffraction were obtained by condensation of pentane into a benzene solution (**4a**) or by evaporation of solvent from a benzene solution of **4b** at 5 °C. The crystals were encapsulated in a glass capillary, which then was placed on the Enraf-Nonius CAD4 diffractometer. The cell parameters were then refined on the basis of 25 reflections chosen from diverse regions of reciprocal space. Parameters and other crystallographic data are summarized in Table I. Intensity data collection by ω (**4a**) and ω–2θ scans (**4b**), respectively.

The structures were solved by direct methods (SHELXS) with full-matrix least-squares refinement of *F*. All atoms were anisotropically refined. Hydrogens were placed in calculated positions (d(C–H) = 0.95 Å) and refined riding on attached carbons. All computations were carried out using a VAX computer with Enraf-Nonius SDP/VAX programs.[9] Scattering factors including f' and f'' were taken from ref 10.

Materials and Methods. $Cp^*(OC)_3W-H$ was prepared according to ref 11. $Me_2Si(H)Cl$, $MeSi(H)Cl_2$, and $HSiCl_3$ were gifts of Wacker Chemie, Burghausen, Germany, and Bayer AG, Leverkusen, Germany. All reactions were conducted under an atmosphere of N_2. Silanes were purified by distillation and evacuation at −78 °C for removal of HCl. *n*-BuLi and $LiAlH_4$ were obtained commercially. Cyclohexane, pentane, toluene, benzene, and diethyl ether were dried by destillation from $LiAlH_4$ under N_2.

Preparation of $Cp^*(OC)_2(Me_3P)W-H$ (1). A 134-mg amount (1.76 mmol) of PMe_3 is added to a solution of 682 mg (1.69 mmol) of $Cp^*(OC)_3W-H$ in 20 mL of benzene. The reaction mixture is irradiated under vigorous stirring for at least 5 h or until gas evolution has ceased. Benzene and excess PMe_3 are removed under vacuum. The remaining oily residue is treated with pentane (2 × 10 mL) until solidification occurs. The solid material is extracted with toluene (3 × 10 mL), and the extract is evaporated to dryness in vacuo. The residue is washed at −30 °C with pentane (3 × 5 mL) separating oily side products to yield **1** as a yellow crystalline powder. Yield: 558 mg (73%) (mp = 79 °C). Anal. Calcd for $C_{15}H_{25}O_2PW$ (**1**): C, 39.84; H, 5.57. Found: C, 39.68; H, 5.52.

^{1}H-NMR (60 MHz/C_6D_6): δ = 2.03 ppm [s, 15H, $C_5(CH_3)_5$], 1.26 ppm [d, ^2J(HCP) = 8.7 Hz, 9H, $P(CH_3)_3$], −7.33 ppm [d, ^1J(HW) = 68.0 Hz]. ^{31}P-NMR (90 MHz/C_6D_6): δ = −18.14 ppm [s, ^1J(PW) = 263.1 Hz]. IR (Pentane): ν(CO) = 1932 (vs), 1853 (vs) cm^{-1}.

Preparation of $Li[W(CO)_2(PMe_3)Cp^*]$ (2). A 2-mL volume (5 mmol) of a 2.5 M solution of *n*-BuLi in hexane is added dropwise to a solution of 1.98 g (4.38 mmol) of $(C_5Me_5)(OC)_2(Me_3P)W-H$ in 60 mL of pentane under vigorous stirring. After 30 min **2** precipitates as a yellow solid, which is separated, washed with pentane, and dried in vacuo. Yield: 1.8 g (90%) of an intensively yellow, extremely pyrophoric powder.

^{1}H-NMR (400 MHz/d_8-THF): δ = 2.03 ppm [s, 15H, $C_5(CH_3)_5$], 1.41 ppm [d, ^2J(HCP) = 7.1 Hz, $P(CH_3)_3$]. ^{13}C-NMR ((50.3 MHz/d_8-THF): δ = 241.71 ppm [d, ^2J(CWP) = 4.2 Hz, ^1J(CW) = 208.2 Hz, CO], 97.18 ppm [s, $C_5(CH_3)_5$], 25.96 ppm [d, ^1J(CP) = 25.7 Hz, $P(CH_3)_3$], 12.61 ppm [s, $C_5(CH_3)_5$]. ^{31}P-NMR (36.3 MHz/d_8-THF): δ = −14.41 ppm [s, ^1J(PW) = 454.2 Hz]. IR (THF): ν(CO) = 1770 (vs), 1640 (vs) cm^{-1}.

Preparation of $Cp^*(OC)_2(Me_3P)W-SiR_3$ (SiR_3 = $Si(H)Me_2$ (3a), $Si(H)(Cl)Me$ (3b), $Si(H)Cl_2$ (3c)). A 3 mmol amount of chlorosilanes $Me_2Si(H)Cl$, $MeSi(H)Cl_2$, and $HSiCl_3$ is added dropwise to a suspension of 505 mg (1.10 mmol) of $Li[W(CO)_2(PMe_3)Cp^*]$ (**2**) in 40 mL of cyclohexane. During this procedure the reaction mixture became ocher. After the mixture is stirred for 1 d, all volatile materials are removed under vacuum. The residue is treated repeatedly with 5 mL of toluene. Evaporation of the united extracts under vacuum to 0.5 mL leads to crystallization of **3a–c**, which are separated. The solid residue is washed at −30 °C with pentane (3 × 5 mL) separating oily side products. This workup affords **3a–c** as yellow to ocher crystalline powders. Yield: 487 mg (87%) (**3a**) (mp = 73 °C), 422 mg (72%) (**3b**) (mp = 73 °C), 410 mg (68%) (**3c**) (mp = 64 °C). Anal. Calcd for $C_{17}H_{31}O_2PSiW$ (**3a**): C, 40.01; H, 6.27. Found: C, 39.86; H, 6.15. Calcd for $C_{16}H_{28}ClO_2PSiW$ (**3b**): C, 36.21; H, 5.32. Found: C, 35.85; H, 5.47. Calcd for $C_{15}H_{25}Cl_2O_2PSiW$ (**3c**): C, 32.69; H, 4.57. Found: C, 33.12; H, 4.26.

3a. ^{1}H-NMR (200 MHz/C_6D_6): δ = 4.76 ppm [sept-d, ^3J(HSiCH) = 3.6 Hz, ^3J(HSiWP) = 2.0 Hz, ^1J(SiH) = 173.7 Hz, 1H, SiH], 1.74 ppm [s, 15H, $C_5(CH_3)_5$], 0.89 ppm [d, ^3J(HCSiH) = 3.6 Hz, 6H, $(H_3C)_2Si$], 1.26 ppm [d, ^2J(HCP) = 8.9 Hz, 9H, $P(CH_3)_3$]. ^{13}C-NMR (50.3 MHz/C_6D_6): δ = 231.1 ppm [d, ^2J(CWP) = 20.0 Hz, ^1J(CW) = 152.9 Hz, CO], 100.40 ppm [s, $C_5(CH_3)_5$], 20.42 ppm [d, ^1J(CP) = 33.4 Hz, $P(CH_3)_3$], 11.12 ppm [s, $C_5(CH_3)_5$], 1.83 ppm [s, $(H_3C)Si$]. ^{31}P-NMR (36.3 MHz/C_6D_6): δ = −13.45 ppm [s, ^1J(PW) = 294.9 Hz]. ^{29}Si-NMR (17.8 MHz/C_6D_6): δ = 7.40 ppm [d, ^2J(SiWP) = 11.7 Hz, ^1J(SiW) = 41.8 Hz].

3b. ^{1}H-NMR (60 MHz/C_6D_6): δ = 6.34 ppm [q, ^3J(HSiCH) = 3.2 Hz, ^1J(SiH) = 208.0 Hz, 1H, SiH], 1.75 ppm [d, ^4J(HCCWP) = 0.5 Hz, 15H, $C_5(CH_3)_5$], 1.31 ppm [d, ^3J(HCSiH) = 3.2 Hz, 3H, $(H_3C)Si$], 1.18 ppm [d, ^2J(HCP) = 9.0 Hz, 9H, $P(CH_3)_3$]. ^{13}C-NMR (100.6 MHz/$CDCl_3$): δ = 232.36 ppm [d, ^2J(CWP) = 21.9 Hz, ^1J(CW) = 148.0 Hz, CO], 102.23 ppm [s, $C_5(CH_3)_5$], 19.44 ppm [d, ^1J(CP) = 34.6 Hz, $P(CH_3)_3$], 12.64 ppm [s, $(H_3C)Si$], 11.35 ppm [s, $C_5(CH_3)_5$]. ^{31}P-NMR (36.3 MHz/C_6D_6): δ = −15.40 ppm [s, ^1J(PW) = 273.4 Hz]. ^{29}Si-NMR (17.8 MHz/C_6D_6): δ = 58.32 ppm [d, ^2J(SiWP) = 15.4 Hz, ^1J(SiW) = 64.1 Hz].

3c. ^{1}H-NMR (200 MHz/C_6D_6): δ = 6.83 ppm [d, ^3J(HSiWP) = 2.2 Hz, ^1J(SiH) = 239.5 Hz, 1H, SiH], 2.25 ppm [s, 15H, $C_5(CH_3)_5$], 1.88 ppm [d, ^2J(HCP) = 9.3 Hz, 9H, $P(CH_3)_3$]. ^{13}C-NMR (50.3 MHz/$CDCl_3$): δ = 229.11 ppm [d, ^2J(CWP) = 23.1 Hz, ^1J(CW) = 143.5 Hz, CO], 101.54 ppm [s, $C_5(CH_3)_5$], 18.86 ppm [d, ^1J(CP) = 35.3 Hz, $P(CH_3)_3$], 10.35 ppm [s, $C_5(CH_3)_5$]. ^{31}P-NMR (36.3 MHz/C_6D_6): δ = −15.20 ppm [s, ^1J(PW) = 256.6 Hz]. ^{29}Si-NMR (17.8 MHz/C_6D_6): δ = 60.87 ppm [d, ^2J(SiWP) = 14.7 Hz]. IR (cyclohexane): ν(CO) = 1929 (m), 1855 (vs) cm^{-1}; ν(SiH) = 2099 (vw) cm^{-1}.

Preparation of $Cp^*(OC)_2(Me_3P)W-SiR_3$ (SiR_3 = $Si(H)_2Me$ (4a), SiH_3 (4b)). To a solution of 1.10 g (2.07 mmol)/278 mg (0.50 mmol) of $Cp^*(OC)_2(Me_3P)W-Si(H)(Cl)Me$ (**3b**)/$Cp^*(OC)_2(Me_3P)W-Si(H)Cl_2$ (**3c**) in 150 mL/30 mL of diethyl ether and 20 mL/5 mL of toluene are added 450 mg (11.86 mmol)/100 mg (2.64 mmol) of $LiAlH_4$ within 15 min at −78 °C. After stirring of the solution for 2 h at the same temperature, the reaction mixture is warmed to room temperature within ½ h. The volatile materials are removed under vacuum, and the remaining

(8) Zimmerer, N.; Kiefer, W. *Appl. Spectrosc.* **1974**, *28*, 279.
(9) *Structure Determination Package*; Enraf-Nonius: Delft, The Netherlands, 1984.
(10) *International Tables for X-ray Crystallography*; Kynoch Press: Birmingham, England, 1974; Vol. IV.
(11) King, R. B.; Fronzaglia, A. *Inorg. Chem.* **1966**, *5*, 1837.

residue is repeatedly treated with 10 mL of toluene. The united extracts were reduced to a volume of ca. 2 mL under vacuum. Cooling to −78 °C affords yellow crystals of **4a,b**, which were purified by recrystallization from toluene. Yield: 887 mg (87%) of **4a** (mp = 101 °C), 219 mg (90%) of **4b** (mp = 87 °C), yellow crystalline powders. Anal. Calcd for $C_{16}H_{29}O_2PSiW$ (**4a**): C, 38.72; H, 5.89. Found: C, 38.93; H, 5.63. Calcd for $C_{15}H_{27}O_2PSiW$ (**4b**): C, 37.36; H, 5.64. Found: C, 37.14; H, 5.59.

4a. ^{1}H-NMR (200 MHz/C_6D_6): δ = 4.22 ppm [qd, ^3J(HSiCH) = 4.2 Hz, ^3J(HSiWP) = 2.0 Hz, ^1J(SiH) = 175.1 Hz, 2H, SiH], 1.73 ppm [s, 15H, $C_5(CH_3)_5$], 1.29 ppm [d, ^2J(HCP) = 8.8 Hz, 9H, $P(CH_3)_3$], 0.76 ppm [t, ^3J(HCSiH) = 4.2 Hz, 3H, $(H_3C)Si$]. ^{13}C-NMR (100.6 MHz/C_6D_6): δ = 229.75 ppm [d, ^2J(CWP) = 20.3 Hz, ^1J(CW) = 151.7 Hz, CO], 99.88 ppm [s, $C_5(CH_3)_5$], 20.47 ppm [d, ^1J(CP) = 34.3 Hz, $P(CH_3)_3$], 10.64 ppm [s, $C_5(CH_3)_5$], −3.54 ppm [s, $(H_3C)Si$]. ^{31}P-NMR (36.3 MHz/C_6D_6): δ = −13.85 ppm [s, ^1J(PW) = 285.7 Hz]. ^{29}Si-NMR (17.8 MHz/C_6D_6): δ = 10.35 ppm [d, ^2J(SiWP) = 12.5 Hz, ^1J(SiW) = 45.8 Hz].

4b. ^{1}H-NMR (200 MHz/C_6D_6): δ = 4.26 ppm [d, ^3J(HSiWP) = 0.4 Hz, ^1J(SiH) = 180.2 Hz, 3H, SiH], 1.72 ppm [d, ^4J(HCCWP) = 0.5 Hz, 15H, $C_5(CH_3)_5$], 1.24 ppm [d, ^2J(HCP) = 9.0 Hz, 9H, $P(CH_3)_3$]. ^{13}C-NMR (50.3 MHz/C_6D_6): δ = 227.34 ppm [d, ^2J(CWP) = 18.1 Hz, ^1J(CW) = 150.1 Hz, CO], 100.00 ppm [s, $C_5(CH_3)_5$], 20.13 ppm [d, ^1J(CP) = 33.2 Hz, $P(CH_3)_3$], 10.66 ppm [s, $C_5(CH_3)_5$]. ^{31}P-NMR (36.3 MHz/C_6D_6): δ = −13.92 ppm [s, ^1J(PW) = 278.3 Hz]. ^{29}Si-NMR (17.8 MHz/C_6D_6): δ = −43.18 ppm [d, ^2J(SiWP) = 13.2 Hz, ^1J(SiW) = 49.8 Hz].

Preparation of $Cp^*(OC)_2(Me_3P)W$–CH_3 (6). $Cp^*(OC)_2(Me_3P)W$–CH_3 (**6**) is prepared from 686 mg (1.50 mmol) of $Li[W(CO)_2(PMe_3)Cp^*]$ (**2**) and methyl iodide (446 mg, 3.14 mmol) following the procedure described for **3a–c**. Yield: 531 mg (76%) (mp = 128 °C), orange crystalline powder. Anal. Calcd for $C_{16}H_{27}O_2PW$ (**6**): C, 41.22; H, 5.84. Found: C, 40.99; H, 5.75.

^{1}H-NMR (200 MHz/C_6D_6): δ = 1.72 ppm [d, ^4J(HCCWP) = 0.5 Hz, 15H, $C_5(CH_3)_5$], 1.06 ppm [d, ^2J(HCP) = 8.3 Hz, 9H, $P(CH_3)_3$], −0.09 ppm [d, ^3J(HCWP) = 13.0 Hz, 3H, WCH_3]. ^{13}C-NMR (100.6 MHz/C_6D_6): δ = 251.77 ppm [d, ^2J(CWP) = 19.8 Hz, ^1J(CW) = 135.3 Hz, CO], 100.42 ppm [s, $C_5(CH_3)_5$], 16.48 ppm [d, ^1J(CP) = 30.6 Hz, $P(CH_3)_3$], 10.67 ppm [s, $C_5(CH_3)_5$], −22.31 ppm [d, ^2J(CWP) = 19.3 Hz, ^1J(CW) = 41.9 Hz, WCH_3]. ^{31}P-NMR (36.3 MHz/C_6D_6): δ = −20.43 ppm [s, ^1J(PW) = 278.3 Hz].

Results and Discussion

Besides oxidative addition of hydrosilanes to transition metal complexes,[2] alkali salt elimination[5] still provides an important method for the preparation of metallosilanes L_nM–SiR_3. For the synthesis of the tungsten–silanes of the type $Cp^*(OC)_2(Me_3P)W$–SiR_3 two routes can be taken into account. One starts with the silyltricarbonyltungsten species $Cp^*(OC)_3W$–SiR_3 generated via the alkali salt metalation route followed by CO/PMe_3 exchange (a); the other directly produces the desired tungsten–silane from the metal anion $[W(CO)_2(PMe_3)Cp^*]^-$ and the corresponding chlorosilane. Previous investigations showed that the ligand-exchange process at the metal in context with (a) cannot be realized even at higher temperature. Attempts to initiate this process by UV light lead to rapid W–Si bond rupture. However, (b) proves to be a profitable way. The lithium metalate can be prepared by reaction of the phosphine-substituted metal hydride **1** with an equimolar amount *n*-BuLi in cyclohexane as a bright yellow, extremely pyrophoric powder (eq 1). Further investigations on related metalates, with regard to reactivity and spectroscopy, are in progress.

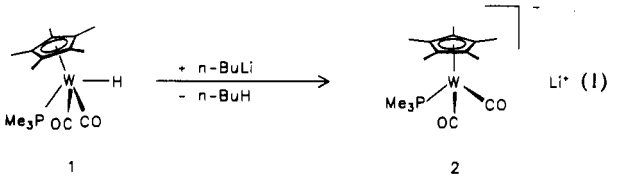

1 2

Heterogenous reaction of $Li[W(CO)_2(PMe_3)Cp^*]$ (**2**) with the corresponding chlorosilanes in cyclohexane results in the formation of the novel silyltungsten complexes **3a–c** within at most 1 day (eq 2). The reactivity of the silanes is found to increase

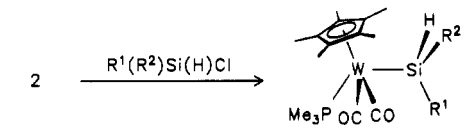

3	a	b	c
R^1	Me	Me	Cl
R^2	Me	Cl	Cl

due to higher chlorine content, i.e. with increasing electrophilicity at the silicon center. Likewise, formation of the byproduct $Cp^*(OC)_2(Me_3P)W$–H (**1**) is enhanced in the same order (up to 10%). The solubility in nonpolar solvents decreases from **3a** to **3c**. The novel complexes **3a–c** are yellow (**3a,b**) to ocher (**3c**) crystalline materials with remarkable air stability in the solid state.

The stabilizing ligands PMe_3 and C_5Me_5, established in the coordination sphere of the tungsten–silanes, now allow an easy Cl/H exchange at the silicon. Treatment of **3b,c** with $LiAlH_4$ in diethyl ether results in the formation of the extraordinarily stable, yellow crystals **4a,b** (eq 3). As already pointed out, previous

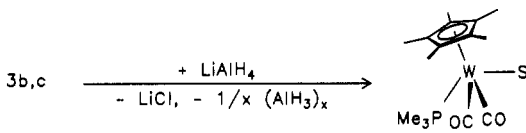

4	a	b
R	Me	H

experiments showed that, even at −78 °C, the tricarbonyl complexes $Cp(OC)_3W$–$Si(H)Cl_2$ and $Cp^*(OC)_3W$–$Si(H)Cl_2$ were cleaved by $LiAlH_4$ into SiH_4 and $Li[W(CO)_3Cp]$ or $Li[W(CO)_3Cp^*]$, respectively.[12] In contrast to that, no evidence for W–Si bond cleavage by treatment with an excess of $LiAlH_4$ has been found in **3a–c** and **4a,b**, even at room temperature. However, **4a,b** decompose slowly in solution when exposed to light.

Crystal Structures. The crystal structures of $Cp^*(OC)_2(Me_3P)W$–$Si(H)_2Me$ (**4a**) and $Cp^*(OC)_2(Me_3P)W$–SiH_3 (**4b**) have been determined. **4a** crystallizes on condensation of pentane into a benzene solution. Suitable single crystals of **4b** were obtained by slow evaporation of a saturated benzene solution at 5 °C. The yellow crystals of **4a,b** were encapsulated in a glass capillary under N_2. Views of the molecules are shown in Figures 1 and 2. Table I contains crystal and diffraction data. Selected bond distances and angles are summarized in Tables II and III. Tables IV and V give listings of non-hydrogen atom positional parameters and isotropic thermal parameters.

The structure determinations for **4a,b** reveal that the ligands occupy a pseudo-square-pyramidal coordination at the central tungsten atom with the Cp* ligand in the axial position (Figures 1 and 2). The C1–W–C2 bond angle between the trans-positioned carbon atoms of the carbonyl groups at the tungsten atom amounts to 107.6 (2)° (**4a**) and 105.8 (4)° (**4b**), respectively. The P–W–Si angle between the silyl substituent and the trans-positioned Me_3P ligand in **4a** was found to be 124.2 (5)°. In **4b** it increases slightly to 126.72 (9)°, presumably because of the reduced steric interaction of the SiH_3 group with the Cp* ligand. Due to the steric congestion of the Cp* ligand in **4a** the methyl group at the silicon is pushed into the spatially favorable anti position to it (torsion angle value Z–W–Si–C3 = 171.98 (22)°, where Z is the

(12) Wekel, H.-U. Doctoral Thesis, University of Würzburg, 1984.

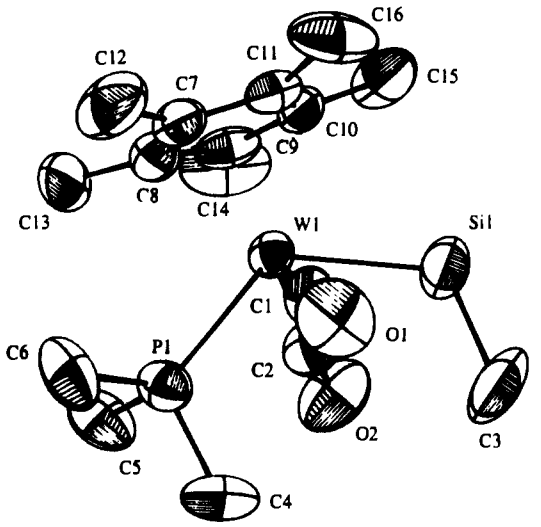

Figure 1. ORTEP[30] drawing of the $Cp^*(OC)_2(Me_3P)W$–$Si(H)_2Me$ complex (**4a**) showing atom numbering. Non-hydrogen atoms are represented by 50% probability ellipsoids.

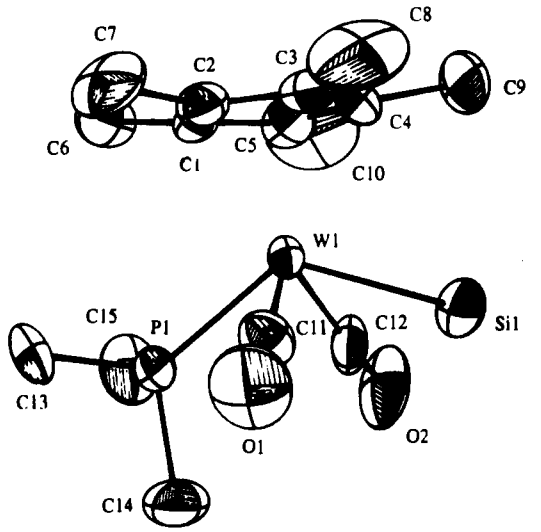

Figure 2. ORTEP[30] drawing of the $Cp^*(OC)_2(Me_3P)W$–SiH_3 complex (**4b**) showing atom numbering. Non-hydrogen atoms are represented by 50% probability ellipsoids.

center of the Cp* unit). Moreover, H_3C4 at the phosphorus and H_3C3 at the silicon adopt a position right between the two carbonyl groups (see Table II) giving rise to an eclipsed conformation ($\angle$C4–P–W–Si–C3 = –2.65 (56)°). In comparison with the ideal tetrahedron the W–Si–C3 angle is markedly widened up to 117.1 (3)° in **4a**. Despite this situation the W–Si distances 2.559 (2) Å (**4a**) and 2.533 (3) Å (**4b**) are significantly longer than the expected value of 2.474 Å.[13] Substitution of the Si-methyl group in **4a** by a hydrogen atom (**4b**) results in a slight decrease of the W–Si distance (about 0.026 Å) reflecting the stronger inductive –I effect of the SiH_3 group. This effect can also be recognized in the slightly enhanced coupling constant ^1J(SiW) of **4b** in comparison with **4a** in the ^{29}Si-NMR spectra (see below). Taking the values of 2.434 (1) Å (**4a**) and 2.441 (2) Å (**4b**), the W–P bond distance is similar to those observed for phosphane-substituted tungsten complexes.[14]

(13) (a) Pauling, L. *The Nature of the Chemical Bond*; Verlag Chemie: Weinheim, Germany 1964. (b) Sutton, L., Ed. *Tables of Interatomic Distances and Configurations in Molecules and Ions*; Spec. Publ. 11, 18; The Chemical Society: London, 1965. (c) Greenwood, N. N.; Earnshaw, A. E. *Chemistry of the Elements*; Pergamon Press: Oxford, U.K., 1984.

(14) (a) Jörg, K. Doctoral Thesis, University of Würzburg, 1986. (b) Hofmockel, U. Doctoral Thesis, University of Würzburg, 1987.

Table II. Selected Structural Parameters for $Cp^*(OC)_2(Me_3P)W$–$Si(H)_2Me$ (**4a**)

Selected Bond Distances (Å)[a]

W1–P1	2.434 (1)	P1–C4	1.822 (6)	C7–C8	1.384 (7)
W1–Si1	2.559 (2)	P1–C5	1.816 (6)	C7–C11	1.424 (7)
W1–C1	1.952 (6)	P1–C6	1.833 (6)	C7–C12	1.536 (8)
W1–C2	1.967 (5)	Si1–C3	1.891 (7)	C8–C9	1.422 (7)
W1–C7	2.366 (5)	O1–C1	1.164 (6)	C8–C13	1.501 (8)
W1–C8	2.384 (5)	O2–C2	1.142 (5)	C9–C10	1.422 (7)
W1–C9	2.390 (5)	W1–C10	2.365 (5)	C9–C14	1.509 (7)
W1–C11	2.345 (5)	C10–C11	1.454 (7)	C10–C15	1.510 (7)

Selected Bond Angles (deg)[a]

P1–W1–Si1	124.2 (5)	C1–W1–C2	107.6 (2)	C4–P1–C6	102.9 (3)
P1–W1–C1	78.3 (2)	W1–P1–C4	114.1 (2)	C5–P1–C6	100.6 (3)
P1–W1–C2	77.4 (2)	W1–P1–C5	118.0 (2)	W1–Si1–C3	117.1 (3)
Si1–W1–C1	70.4 (2)	W1–P1–C6	117.4 (2)	W1–C1–O11	176.5 (5)
Si1–W1–C2	70.1 (2)	C4–P1–C5	101.4 (3)	W1–C2–O21	177.8 (6)

Selected Torsion Angle (deg)[a]

Z–W–Si–C3	171.98 (22)[b]	C3–Si–W–C2	–65.18823
C4–P–W–Si–C3	–2.65 (56)	C4–P–W–C1	–52.39270
C3–Si–W–C1	52.039	C4–P–W–C2	58.88449

[a] Numbers in parentheses are estimated standard deviations in the least significant digits. [b] Z is center of the Cp* unit.

The compounds crystallize in space groups *Pbca* (**4a**) and $P2_12_12_1$ (**4b**), which correspond to factor groups D_{2h}^{15} and D_2^4, respectively. A factor group analysis and a vibrational study of the crystalline materials are in work.[15]

NMR Spectra. The bonding situation of the systems studied can be well described by NMR and vibrational spectra. With regard to the NMR studies the existence of the NMR-active isotope ^{183}W proves to be very helpful (nuclear spin $I = {}^1/_2$, natural abundance 14.4%): The ^{29}Si-NMR data (nuclear spin $I = {}^1/_2$, natural abundance of ^{29}Si 4.7%) reveal that successive substitution of silicon-attached methyl groups by chlorine effects downfield shifts (7.40 (**3a**), 58.32 (**3b**), 60.87 ppm (**3c**)) with the most remarkable leap occurring in going from **3a** to **3b**. However, introduction of hydrogen atoms implies a different effect. The most negative $\delta(^{29}Si)$ value, –43.18 ppm, is observed for **4b**, reflecting the considerable electronic shielding at the silicon.

Of great interest with respect to the characterization of the W–Si bond are the coupling constants ^1J(SiW) in the ^{29}Si-NMR spectra, since the size of the coupling constants directly reflects the s bond order of the σ-bond between the coupling nuclei. Usually ^1J(SiW) increases when strongly electronegative substituents—here Cl (cf.: **3a**, ^1J(SiW) = 41.8 Hz; **3b**, ^1J(SiW) = 64.1 Hz; ^1J(SiW) of **3c** was not available due to solubility problems)—are introduced. However, one can notice its increase with hydrogen substitution from **3a** (41.8 Hz) to **4a** (45.8 Hz) and **4b** (49.8 Hz). This may be considered as being due to W–Si bond length variations, as the crystal structure determinations of **4a,b** reveal that additional introduction of silicon-attached hydrogens effects some reduction of the W–Si bond distance (**4a**, d(W–Si) = 2.559 (2) Å; **4b**, d(W–Si) = 2.533 (3) Å).

The bond relations expressed by the coupling constants ^1J(SiW) can be correlated with ^1J(PW) in the ^{31}P-NMR spectra and ^1J(CW) in the ^{13}C-NMR spectra in a characteristic manner. Accordingly, the increase of electron density between tungsten and silicon effects both weakening of the W–P (decrease of ^1J(PW) in the order **3a** (294.9), **3b** (273.4), **3c** (256.6 Hz) and the W–CO bonds (decrease of ^1J(CW) in the order **3a** (152.9), **3b** (148.0), **3c** (143.5 Hz)). The $\delta(^{31}P)$ values migrate in the order **3a,b,c** only insignificantly from –13.45 to –15.40 and –15.20 ppm, respectively. Hence, the weaker the W–P bond, the greater the electron density located on the phosphorus. In accordance with that, one can notice the increase of the coupling constants ^2J(HCP) in the ^{1}H-NMR spectra (8.9 Hz (**3a**), 9.0 Hz (**3b**), 9.3 Hz (**3c**)).

The increase of ^1J(SiH) when Cl is substituted for methyl groups in the series **3a** → **3b** → **3c** (^1J(SiH) = 173.7, 208.0, and

(15) Posset, U.; Kiefer, W. To be published.

Table III. Selected Structural Parameters for $Cp^*(OC)_2(Me_3P)W-SiH_3$ (**4b**)

		Bond Distances (Å)[a]			
W1–P1	2.441 (2)	W1–C12	1.945 (8)	C1–C6	1.51 (1)
W1–Si1	2.533 (3)	P1–C13	1.80 (1)	C2–C3	1.42 (1)
W1–C1	2.366 (9)	P1–C14	1.84 (1)	C2–C7	1.52 (1)
W1–C2	2.346 (9)	P1–C15	1.81 (1)	C3–C4	1.41 (1)
W1–C3	2.324 (7)	O1–C11	1.17 (1)	C3–C8	1.52 (2)
W1–C4	2.340 (9)	O2–C12	1.17 (1)	C4–C5	1.41 (1)
W1–C5	2.35 (1)	C1–C2	1.41 (1)	C4–C9	1.51 (1)
W1–C11	1.962 (9)	C1–C5	1.43 (1)	C5–C10	1.52 (2)
		Selected Bond Angles (deg)[a]			
P1–W1–Si1	126.72 (9)	C11–W1–C12	105.8 (4)	C13–P1–C15	100.8 (6)
P1–W1–C11	78.6 (3)	W1–P1–C13	117.7 (4)	C14–P1–C15	101.8 (5)
P1–W1–C12	77.8 (3)	W1–P1–C14	114.3 (4)	W1–C11–O1	176 (1)
Si1–W1–C11	71.4 (3)	W1–P1–C15	118.6 (4)	W1–C12–O2	174 (1)
Si1–W1–C12	69.8 (3)	C13–P1–C14	100.9 (5)	C1–C2–C3	106.6 (8)

[a] Numbers in parentheses are estimated standard deviations in the least significant digits.

Table IV. Non-Hydrogen Atom Positional Parameters and Their Esd's for $Cp^*(OC)_2(Me_3P)W-Si(H)_2Me$ (**4a**)

atom	x	y	z	B_{eq} (Å²)[a]
W1	0.01182 (2)	0.70486 (2)	0.36039 (2)	3.465 (6)
P1	–0.1234 (2)	0.6079 (2)	0.3746 (1)	4.61 (6)
Si1	0.0255 (2)	0.8565 (2)	0.4184 (2)	5.83 (7)
O1	–0.1503 (5)	0.8248 (6)	0.3044 (5)	7.4 (2)
O2	–0.0021 (8)	0.6885 (7)	0.5267 (4)	9.0 (3)
C1	–0.0915 (7)	0.7793 (7)	0.3272 (6)	4.8 (2)
C2	0.0010 (8)	0.6943 (8)	0.4655 (5)	5.7 (3)
C3	–0.082 (1)	0.900 (1)	0.4666 (9)	10.5 (4)
C4	–0.2202 (8)	0.655 (1)	0.4261 (8)	8.7 (4)
C5	–0.1057 (9)	0.5046 (8)	0.4214 (6)	6.9 (3)
C6	–0.1821 (8)	0.5695 (8)	0.2926 (7)	6.7 (3)
C7	0.0723 (7)	0.6576 (7)	0.2483 (6)	4.5 (2)
C8	0.0997 (7)	0.5952 (7)	0.2982 (6)	4.8 (2)
C9	0.1621 (7)	0.6352 (7)	0.3482 (5)	5.0 (2)
C10	0.1723 (6)	0.7251 (7)	0.3295 (5)	4.5 (2)
C11	0.1148 (7)	0.7395 (7)	0.2658 (5)	4.3 (2)
C12	0.015 (1)	0.641 (1)	0.1794 (6)	7.9 (4)
C13	0.0831 (9)	0.4980 (8)	0.2949 (9)	9.0 (4)
C14	0.2159 (9)	0.589 (1)	0.4073 (7)	9.3 (4)
C15	0.2407 (8)	0.791 (1)	0.3613 (8)	9.6 (4)
C16	0.1135 (9)	0.8242 (9)	0.2239 (7)	7.9 (3)

[a] The form of the isotropic equivalent temperature factor is $B_{eq} = (4/3)[a^2B(1,1) + b^2B(2,2) + c^2B(3,3) + ab(\cos\gamma)B(1,2) + ac(\cos\beta)B(1,3) + bc(\cos\alpha)B(2,3)]$.

Table V. Non-Hydrogen Atom Positional Parameters and Their Esd's for $Cp^*(OC)_2(Me_3P)W-SiH_3$ (**4b**)

atom	x	y	z	B_{eq} (Å²)[a]
W1	0.24614 (4)	0.82566 (2)	0.23231 (2)	2.258 (4)
P1	0.1532 (3)	0.9259 (2)	0.1143 (2)	3.54 (5)
Si1	0.4776 (3)	0.8526 (2)	0.3281 (2)	4.95 (6)
O1	0.5304 (9)	0.8326 (8)	0.1082 (6)	7.8 (2)
O2	0.211 (1)	1.0132 (5)	0.3306 (5)	7.6 (2)
C1	0.031 (1)	0.7293 (6)	0.2169 (6)	3.9 (2)
C2	0.160 (1)	0.6777 (6)	0.1930 (6)	4.0 (2)
C3	0.250 (1)	0.6698 (5)	0.2703 (6)	4.4 (2)
C4	0.179 (1)	0.7175 (7)	0.3407 (6)	4.4 (2)
C5	0.043 (1)	0.7557 (7)	0.3075 (7)	4.5 (2)
C6	–0.112 (1)	0.7402 (9)	0.1628 (9)	7.8 (3)
C7	0.180 (2)	0.6274 (8)	0.1054 (8)	7.6 (4)
C8	0.393 (2)	0.6107 (7)	0.278 (1)	9.7 (5)
C9	0.226 (2)	0.7168 (9)	0.4370 (6)	9.0 (4)
C10	–0.072 (1)	0.805 (1)	0.365 (1)	11.1 (5)
C11	0.425 (1)	0.8337 (7)	0.1557 (6)	4.0 (2)
C12	0.231 (1)	0.9449 (6)	0.2914 (5)	4.5 (2)
C13	0.128 (1)	0.8756 (8)	0.0064 (6)	5.4 (3)
C14	0.279 (1)	1.0238 (7)	0.0879 (8)	7.1 (3)
C15	–0.027 (1)	0.9833 (8)	0.1289 (9)	6.4 (3)

[a] See footnote *a* of Table IV.

239.5 Hz, respectively) is expected from the Bent rule.[16] According to this, a more electronegative substituent (Cl) requires more p-character at the silicon atom for its bonding, leaving more s-character for the other atoms bound to Si as H (and W; see below). An increase (even if a much smaller one) is also observed when substituting hydrogen for methyl groups in the series **3a** → **4a** → **4b** (^1J(SiH) = 173.7, 175.1, and 180.1 Hz, respectively); that is, hydrogen acts as being more electronegative toward Si than the methyl group. This is the way the electronegativity of hydrogen and the methyl group has been described by Bent, but tabulated numerical values[17] would suggest inverted relative positions in the electronegativity series.

The ^{13}C-NMR spectrum of the silyltungsten complex **3b** showed only one single peak for the diastereotopic carbonyl carbons. The frequently[18] different $\delta(^{13}C)$ shifts coincide accidentally, or the molecule might be fluxional.

Vibrational Spectra. Since no detailed vibrational data concerning metal–ligand and intraligand modes are known for silyltungsten complexes of the type described in this paper or related compounds, part of a comprehensive vibrational study on these complexes is presented here.

The compounds **3a,b** and **4a,b** have been investigated by means of difference Raman spectroscopy, which proved to be a most useful tool to analyze the vibrational behavior of this type of complex, especially in the low-frequency region of interest. Additionally, IR spectra of the CO- and SiH-stretching regions have been recorded. Complementary investigations on the methyl derivatives $Cp^*(OC)_3W-CH_3$ (**5**)[19] and $Cp^*(OC)_2(Me_3P)W-CH_3$ (**6**) have been made for comparison purposes. **6** is prepared from $Li[W(CO)_2(PMe_3)Cp^*]$ (**2**) and methyl iodide according to the conditions of eq 2.

Although the total symmetry of the molecules is actually only C_1, the spectra can be evaluated and assigned on the basis of the local symmetry approach[20] and of polarization measurements. The vibrational data are compiled in Table VI, and a representative Raman spectrum of the $-SiH_3$ complex (**4b**) is shown in Figure 3.

C–O Stretching Vibrations. The spectra show the expected two ν(CO) modes of medium (Raman) and high (IR) intensity in each case, with only little changes in frequencies within the silyl series. Polarization data as well as the ratio of IR intensities (I_s:I_{as} < 1) state the local symmetry to be C_s for the carbonyl ligands. Hence, corresponding to the crystal structures of **4a,b**, trans geometry is present for the $W(CO)_2$ unit in all species in solution, too. As expected, both the symmetric and antisymmetric band frequencies move to higher wavenumbers with an increase of electronegativity of the silyl group. The lowering of π-back-

(16) Bent, H. A. *Chem. Rev.* **1961**, *61*, 275.

(17) Huheey, J. E. *Inorganic Chemistry*; W. de Gruyter: Berlin, New York, 1988.

(18) Schmitzer, S.; Malisch, W. To be published.

(19) (a) King, R. B.; Efraty, A.; Douglas, W. M. *J. Organomet. Chem.* **1973**, *60*, 125. (b) King, R. B.; Efraty, A. *J. Am. Chem. Soc.* **1972**, *94*, 3773.

(20) Cotton, F. A.; Liehr, A. D.; Wilkinson, G. *J. Inorg. Nucl. Chem.* **1955**, *1*, 175.

Table VI. Observed Raman Frequencies and IR Absorptions (in Parentheses) of $Cp^*(OC)_2(Me_3P)W$–R Complexes[a]

substituents R					
–CH_3	–SiH_3	–$Si(H)_2Me$	–$Si(H)Me_2$	–Si(H)(Cl)Me	assgnt
	2083 st (2075 w, sh)	2055 st (2055 w)	2031 m (2031 vw)	2074 m (2088 vw)	$\nu(SiH)_s$
	2063 sh, dp (2065 m)	2048 sh, dp			$\nu(SiH)_{as}$
1904 m (1923 vs)	1892 m, dp (1903 s)	1886 m, dp (1899 s)	1881 m, dp (1893 s)	1901 st, dp (1907 s)	$\nu(CO)_s$
1815 m, dp (1837 vs)	1814 m, dp (1832 vs)	1805 m, dp (1827 vs)	1803 m, dp (1821 vs)	1818 m, dp (1832 vs)	$\nu(CO)_{as}$
1418 st, p	1420 st, p	1417 st, p	1419 st, p	1418 st, p	$\delta(CH_3)_s$
721 m, dp	727 m, dp	725 m, dp	724 m, dp	728 m, dp	$\nu(PC)_{as}$
670 st, p	675 st, p	674 st, p	674 st, p	675 st, p	$\nu(PC)_s$
			646 m, p		$\nu(SiC)_s$
629 vw	624 w, dp	624 w, dp	624 w, dp	624 w, dp	δ(WCO)
590 st, p	593 st, p	593 st, p	594 st, p	593 st, p	$\nu(ring)_s$
543 m, dp	545 m, dp	543 m, dp	544 m, dp	544 m, dp	δ(WCO)
514 sh, dp	503 m, dp	503 m, dp	512 m, dp	500 m, dp	$\nu(WC)_{as}$
501 vs, p	473 vs, p	473 vs, p	472 vs, p	469 vs, p	$\nu(WC)_s$
442 s					ν(WMe)
				437 m, p	ν(SiCl)
424 sh	423 w, dp	422 w, dp	423 w, dp	425 sh, dp	
351 m, p	359 m	357 m	359 m	356 m	ν(W–ring)$_s$
	326 st	315 m	307 m	321 m	ν(WSi)
	228 sh	230 m, p	234 sh	247 sh	
219 m, p	221 m, p	218 sh, p	207 m, p	228 m, p	ν(WP)
186 sh			194 sh	200 sh	
174 st	169 m, 140 m, 108 m	169 m, 143 w, 110 w	169 m, 130 sh, 113 m	171 m, 143 w, 111 s	skeletal deformations

[a] Measured in CH_2Cl_2 (Raman) and cyclohexane (IR) solutions (only the most important features are listed). Key: vs, very strong; st, strong; m, medium; w, weak; vw, very weak; sh, shoulder, p, polarized; dp, depolarized; s, symmetric; as, antisymmetric; values in cm^{-1}.

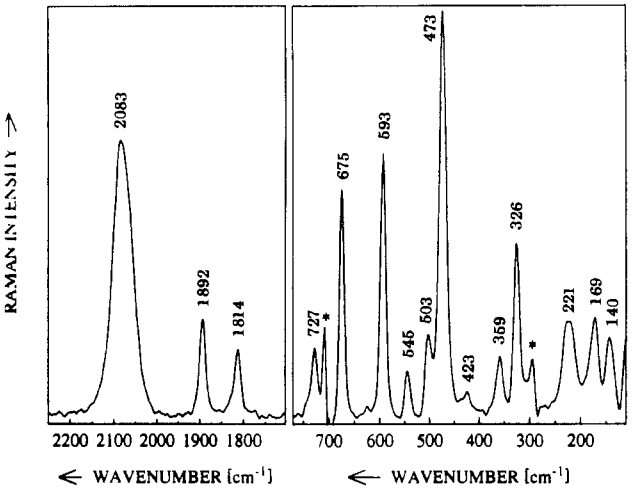

Figure 3. Part of the difference Raman spectra of $Cp^*(OC)_2(Me_3P)W$–SiH_3 (**4b**) in CH_2Cl_2: excitation wavelength λ_0 = 676.442 nm; laser power P = 100 mW; slit width s = 3 cm^{-1}; concentration c = 0.25 mol L^{-1}; temperature = 300 K. Asterisks indicate residual solvent peaks.

bonding into a π^*-MO of the CO leads to the decrease of the ^1J(CW) coupling constants (see above) i.e. to the decrease of electron density within the W–C–O unit. The highest frequencies are observed for the dichlorosilyl derivative **3c** for which strong fluorescence unfortunately prevented the recording of Raman data. The differences of about 10 cm^{-1} (sym) and 18 cm^{-1} (antisym) in IR and Raman values are clearly due to solvent effects.

W–Ligand Stretching Vibrations. Two prominent features are observed in all the Raman spectra in the range between 514 and 469 cm^{-1}, corresponding to the very strong symmetric, polarized ν(WC) mode, accompanied by the far less intense, depolarized antisymmetric vibration about 30 cm^{-1} higher in each case. With the increase of the ν(CO) values, one observes the expected simultaneous lowering of the ν(WC) frequencies, although the frequency shifts are far smaller.

The tungsten–silicon stretching vibration gives rise to a Raman band of varying intensity and low depolarization ratio in the range between 307 and 326 cm^{-1}. Comparisons with already published ν(M–Si) frequencies of silyliron and -cobalt complexes[21] show that there obviously is no mass effect. Hence the frequency of this vibration is mainly determined by the donor/acceptor properties of the transition metal. The relative ν(WSi) band intensities decrease in the order **4b** > **4a** > **3a**. The same order is observed for the decrease of the ν(WSi) frequencies and the corresponding ^1J(WSi) coupling constants (**4b**, 326 cm^{-1}/49.8 Hz; **4a**, 315 cm^{-1}/45.8 Hz; **3a**, 307 cm^{-1}/41.8 Hz). Since Raman data for **3c** are lacking, only the values for **3a,b** can be correlated (**3a**, 307 cm^{-1}/41.8 Hz; **3b**, 321 cm^{-1}/64.1 Hz).

A broad band of medium Raman intensity occuring in the range between 200 and 230 cm^{-1} can be assigned to the ν(WP) stretching vibration. This is in agreement with previous publications of ν(MP) frequencies in related complexes.[22a]

The half-sandwich Cp^*W moiety is ideally of local C_{5v} symmetry and hence expected to give two metal–ring stretching modes of species A_1 and E_1. Both have been reported previously to occur between 300 and 400 cm^{-1} in related Cp complexes.[22b,23] Spectra recorded in this investigation show the corresponding symmetric $\nu(Cp^*W)$ vibration to occur at about 360 cm^{-1} with unusually low intensity and low depolarization ratio. The expected degenerate mode can only be assigned to a very weak shoulder at higher frequencies. The assignment is supported by measurements on the related complexes Cp^*MoO_3[24] and $Cp^*(CO)_3W$–CH_3.[25] With comparison of the spectra of the Cp–W and Cp^*–W moieties, no mass effect is observed for the ring–metal stretching modes. This is in agreement with previous results on benzene and mesitylene complexes.[26]

Ligand Modes. Symmetric PC_3 stretching and Cp^* ring breathing vibrations give rise to highly polarized, strong Raman bands at about 675 and 590 cm^{-1}, respectively. The latter is

(21) Van den Berg, G. C.; Oskam, A. *J. Organomet. Chem.* **1975**, *91*, 1.
(22) (a) Chalmers, A. A.; Lewis, J.; Whyman, R. *J. Chem. Soc. A* **1967**, 1817. (b) Craig, P. J. *Can. J. Chem.* **1970**, *48*, 3089.
(23) (a) Adams, D. M.; Squire, A. *J. Organomet. Chem.* **1973**, *63*, 381. (b) Davidson, G.; Duce, D. A. *J. Organomet. Chem.* **1976**, *120*, 229. (c) Hyams, I. J.; Bailey, R. T.; Lippincott, E. R. *Spectrochim. Acta* **1967**, *23A*, 273.
(24) Polzer, T.; Kiefer, W.; Radius, U.; Sundermeyer, J. To be published.
(25) Polzer, T.; Posset, U.; Kiefer, W. To be published.
(26) (a) Armstrong, R. S.; Aroney, M. J.; Barnes, C. M.; Nugent, K. W. *Appl. Organomet. Chem.* **1990**, *4*, 569. (b) Davidson, G.; Riley, E. M. *Spectrochim. Acta* **1971**, *27A*, 1649. (c) Adams, D. M.; Squire, A. *J. Chem. Soc.* **1970**, 814.

therefore shifted down by about 520 cm^{-1} with respect to the corresponding Cp vibration which can be explained by the mass effect. Previous assignments of the ring modes[27] have proved to be doubtful and must be revised according to our experimental results. A complete vibrational analysis of the Cp* ligand is in work.[28]

Broad and strong Raman bands in the 2000-cm^{-1} region are observed for the hydrosilyl complexes, due to the Si–H stretching vibrations. The corresponding IR absorptions are usually weak but significant. The relatively low ν(SiH) values argue for a strong hydride character of the hydrogen and hence reflect enhanced reactivity in hydrogen/halogen exchange reactions.[5b,c] In comparison with the nonmetalated silanes, the SiH stretching frequencies are generally shifted by about 100 cm^{-1} to lower wavenumbers. Correspondingly, the ^{1}H-NMR spectra of the silyltungsten complexes reveal smaller ^1J(SiH) coupling constants (between 170 and 240 Hz) than those of the precursor silanes. As in the case of the ν(WSi) values, the ν(SiH) frequencies (IR data listed; the same is observed for Raman shifts) and the ^1J(SiH) coupling constants decrease in the order **3c** > **3b** > **3a** (**3c**, 2099 cm^{-1}/239.5 Hz; **3b**, 2088 cm^{-1}/208.0 Hz; **3a**, 2031 cm^{-1}/173.7 Hz) and **4b** > **4a** > **3a** (**4b**, 2075 cm^{-1}/180.2 Hz; **4a**, 2055 cm^{-1}/175.1 Hz; **3a**, 2031 cm^{-1}/173.7 Hz), respectively.

SiCl and $Si–C_2$ stretching modes are located at positions comparable with those of conventional organochlorosilanes.[29]

Conclusion

Silyltungsten complexes of the type $Cp^*(OC)_2(Me_3P)W–SiR_3$ obtained via metalation of chlorosilanes with $Li[W(CO)_2(PMe_3)Cp^*]$ are of considerable interest with respect to substitution reactions at the silicon atom, which according to the results of this paper occur without W–Si bond breaking. As a consequence, a rich chemistry can be predicted referring to ligand-exchange reactions including even strong nucleophiles. The electronic and vibrational behavior of this type of compound can be studied comprehensively on the complexes $Cp^*(OC)_2(Me_3P)W–SiR_3$, which show up to four different NMR-active isotopes and are good Raman scatterers. The most important vibrational modes could be assigned by means of symmetry considerations and polarization measurements. The ^{1}H-, ^{13}C-, ^{31}P-, and ^{29}Si-NMR data are in agreement with the expectations and correlate well with vibrational spectroscopic results. For the most interesting W–Si bond, ^1J(WSi) coupling constants between 41 and 61 Hz are observed. The corresponding stretching vibration gives rise to a polarized Raman band between 307 and 326 cm^{-1}. Pseudo-square-pyramidal coordination at the central atom and trans geometry for the CO ligands are found by X-ray diffraction and IR and Raman data in both the crystal lattice and solution.

Acknowledgment. We gratefully acknowledge financial support from the Deutsche Forschungsgemeinschaft (Sonderforschungsbereich 347, Projects B2 and C2) as well as from the Fonds der Chemischen Industrie.

Supplementary Material Available: Tables of crystallographic data, atomic coordinates and anisotropic thermal parameters, and bond lengths and angles for **4a**,**b** (18 pages). Ordering information is given on any current masthead page.

(27) Butler, I. S.; Harvey, P. D.; McCall, J. M.; Shaver, A. *J. Raman Spectrosc.* **1986**, *17*, 221.
(28) Polzer, T.; Kiefer, W. To be published.
(29) (a) Smith, A. L.; Anderson, D. R. *Appl. Spectrosc.* **1984**, *38*, 822. (b) Durig, J. R.; Hawley, C. W. *J. Chem. Phys.* **1973**, *58*, 237.
(30) Johnson, C. K. *ORTEP-II, A Fortran Thermal Ellipsoid Plot Program for Crystal Structure Illustration*; Report ORNL-5138; National Technical Information Service, U.S. Department of Commerce: Springfield, VA, 1976.